Patient specific Finite Element model of the face soft tissue for computer-assisted maxillofacial surgery

Matthieu Chabanas, Vincent Luboz, Yohan Payan

Patient specific finite element model of the face soft tissues for computer-assisted maxillofacial surgery

Matthieu Chabanas, Vincent Luboz, Yohan Payan *

TIMC-IMAG Laboratory, UMR CNRS 5525, University of Grenoble.
Institut Albert Bonniot, 38706 La Tronche Cedex, France

Abstract

This paper addresses the prediction of face soft tissue deformations resulting from bone repositioning in maxillofacial surgery.

A generic 3D Finite Element model of the face soft tissues was developed. Face muscles are defined in the mesh as embedded structures, with different mechanical properties (transverse isotropy, stiffness depending on muscle contraction). Simulations of face deformations under muscle actions can thus be performed.

In the context of maxillofacial surgery, this generic soft-tissue model is automatically conformed to patient morphology by elastic registration, using skin and skull surfaces segmented from a CT exam. Some elements of the patient mesh could be geometrically distorted during the registration, which disables Finite Element analysis. Irregular elements are thus detected and automatically regularized. This semi-automatic patient model generation is robust, fast and easy to use. Therefore it seems compatible with a clinical use.

Six patient models were successfully built, and simulations of soft tissue deformations resulting from bone displacements performed on two patient models. Both the adequation of the models to the patient morphologies and the simulations of post-operative aspects were qualitatively validated by five surgeons. Their conclusions are that the models fit the morphologies of the patients, and that the predicted soft tissue modifications are coherent with what they would be expecting.

Key words: Computer aided maxillofacial surgery, Finite Element method, Mesh conformation, Elastic registration, Finite Element mesh regularity

* Corresponding authors: {Matthieu.Chabanas,Vincent.Luboz,Yohan.Payan}@imag.fr

1 Introduction

Orthognathic surgery is addressed for patients suffering from maxillofacial dysmorphosis of the lower part of the face, i.e. from a rupture in the equilibrium between the mandible, the upper jaw and the face. This rupture has important consequences: functional, with disruptions of the dental occlusion, and aesthetic, with morphometric criterion that run out of a norm (face asymmetry in the frontal view, excess mandibular growth in the case of mandibular prognathism, etc).

This recent and delicate surgery requires a strong collaboration between surgeons and orthodontists, to build a planning that integrates multiple data gathered from different sources: clinical examination (anthropometry), orthodontia (dental models) and radiology (cephalometry).

This paper presents a complete protocol for computer-aided maxillofacial surgery. The first part of this protocol concerns the planning of bone structures repositioning and was introduced in Bettega et al. (2000). The next part of the protocol, addressed in this paper, is the prediction of the facial aesthetic and functional consequences of the bone repositioning planning. This step is important for the surgeon as the prediction of facial tissue deformations might modify a planning based only on skull and dental analysis. Moreover, one of the main patient requests is a reliable prediction of the post-operative aesthetic aspect.

The first part of this paper introduces our complete surgical planning protocol for orthognatic surgery. A state of the art is then presented and discussed for each step of this protocol. The third part focusses on the consequences of the bone structure repositioning on the facial soft tissues. A modeling framework is introduced, providing the automatic elaboration of a 3D biomechanical face model adapted to each patient morphology. A clinical validation protocol is then defined, based on the qualitative analysis of several specialized surgeons. Results are presented in a fifth part, consisting in six models of patients built with our method, and the simulations of soft tissue deformations following bone repositioning with two of these models. Finally, results and methodology are discussed and a quantitative validation scheme of the complete protocol is proposed.

2 Computer-aided protocol for orthognathic surgery

A computer-aided protocol for orthognathic surgery has been developed since 1995 in strong collaboration with two maxillofacial departments in Grenoble

and Toulouse Hospitals, in France. The complete protocol is presented in this paper.

2.1 Traditional clinical protocol

Orthognathic surgical protocol is usually defined by four steps. The first step is the characterization of the dysmorphosis. This characterization is made by comparing the patient anatomy with functional, morphological and aesthetical norms. Criterions retains for this comparison are (1) the aesthetic equilibrium of the patient face, (2) the dental arches deformities and the teeth occlusion, and (3) the cephalometric analysis. The first criterion is very qualitative and highly depends on the surgeon experience. Dental arches deformities and teeth occlusion are usually evaluated with panoramic radiographies and with plaster casts of the superior and inferior dental arches. The morphometric analysis of the face, called the cephalometric analysis, consists in defining anatomical landmarks on medical images and computing distances and angles out of these landmarks. These measurements are therefore compared to a norm to characterize the patient dysmorphosis (for example, see Delaire (1978)).

The second step of the orthognathic surgical protocol is the definition of the surgical gesture. Following the characterization and analysis of the dysmorphosis, the required osteotomies (upper and/or lower jaw) and the displacements to apply to each bone segment are defined. Traditional clinical protocol This planning is then validated during the third step of the protocol, with a simulation of the surgical gesture. Tracing papers are used to simulate modifications of the cephalometric anatomical landmarks. Teeth plaster casts are manually cut to simulate bone osteotomies and to validate the dental occlusion. Simulations of the consequences of bone repositioning on the facial soft tissues are still very qualitative. For example, some surgeons work on patient photography (front/profile) and try to cut these photography to simulate a modification in bone positioning and to qualitatively predict the patient face aesthetics after surgery.

Finally, the fourth step of the orthognathic surgical protocol is the transfer of the planning to the operating theater. This transfer, achieved using plastic splints and compass, is very delicate. No quantitative per-operative measurements guaranty the defined planning to be followed with accuracy.

2.2 Definition of the Computer-Aided clinical protocol

Many shortcomings in the classical orthognathic clinical protocol may be improved by the use of computer-aided and medical imaging techniques. The

cephalometry, usually built from 2D frontal or sagittal teleradiographies, could be driven in 3D, on a virtual reconstruction of the patient skull. This is especially useful in the case of patients suffering from dismorphosys both in the coronal plane and sagittal plane, which are therefore very difficult to apprehend out of 2D images only. Another important issue concerns the predictions of the aesthetic consequences of the bone repositioning planning. The computer framework could be used to numerically simulate the mechanical behavior of the facial soft tissues in response to the modification of the bones position. Another point is the transfer of the planning into the operating theater. Classical navigation techniques could be used to track the position of surgical tools and to quantitatively measure the displacements applied to the mandible or maxillary. Finally, mathematical and numerical methods could be defined to measure, from medical images, differences between pre-operative and post-operative morphologies, in order to quantitatively compare the surgical gesture with the planning.

To summarize our point of view, six main steps must be fulfilled to define a complete computer-aided clinical protocol:

(1) Bone osteotomies must be simulated on a virtual 3D model of the patient skull in ways that reflect actual surgical procedures
(2) The bone segments should be mobilized with six degrees of freedom
(3) A 3D cephalometric analysis must be integrated to plan the bone segments repositioning
(4) A quantitative measurement of the dental occlusion correction provided by the orthodontist should be integrated into the 3D analysis
(5) The deformations of the patient facial soft tissues resulting from the repositioning of the underlying bone structures should be predicted
(6) The 3D bone-repositioning planning must be transferred to the operating theater, as a computer-aided intervention

2.3 Previous works

The first two issues of the computer-aided clinical protocol have been widely addressed in the literature (Cutting et al., 1986; Marsh et al., 1986; Udupa and Odhner, 1991; Lo et al., 1994; Vannier et al., 1996; Keeve et al., 1996; Teschner et al., 1999; Schutyser et al., 2000; Zachow et al., 2000; Barré et al., 2000; Everett et al., 2000; Xia et al., 2000). Most of these works are based on a 3D reconstruction of the skull from CT exams. They propose interesting interactive tools to cut and manipulate bone segments. However, none of them address neither the third nor the fourth issue, namely the cephalometric planning and the orthodontic analysis traditionally defined by the surgeons.

4

The fifth issue of the protocol has been mainly addressed in two scientific communities. The first face modeling works were proposed by computer animation groups, and were mainly motivated by real-time output with graphically realistic behavior. They were mainly based on a discrete modeling framework, with sparse mass-spring entities regularly assembled inside facial tissues (Lee et al., 1995). Then, the community working on computer aided surgery applied some of these models for plastic and maxillofacial clinical issues (Delingette et al., 1994; Waters, 1996; Keeve et al., 1996; Teschner et al., 1999; Barré et al., 2000). Arguing for the lack of accuracy of discrete models, the difficulty of setting elastic parameters, and the increasing performances of the computers, continuous Finite Element models were then proposed (Keeve et al., 1998; Roth et al., 1998; Schutyser et al., 2000; Zachow et al., 2000). In addition, in order to simulate facial expressions, muscle activation modeling was presented by Lee et al. (1995), Konno et al. (1996) and Lucero and Munhall (1999) using mass-spring models. Similarly, R. M. Koch and Bosshard (1998) use the combination of a polynomial Finite Element surface and a set of springs (representing muscles) attached to the skull. More recently, the integration of muscles in a Finite Element model has been proposed in Gladilin et al. (2001).

In the computer-aided maxillofacial surgery literature, models are used for planning issues, which clearly require accurate modeling of the continuum structure of the tissues. Moreover, unlike in computer animation, real-time computation is not essential. This is why computer aided surgery modeling groups nowadays commonly use continuous modeling based on the Finite Element Method (Keeve et al., 1998; Roth et al., 1998; Schutyser et al., 2000; Zachow et al., 2000; Gladilin et al., 2001). However, these models present many shortcomings from a numerical and mechanical point of view (see part 3.3 for a review). Moreover, none of them except Gladilin et al. (2001) integrate the anisotropic continuous modeling of facial muscles, which is necessary to predict the functional consequences of surgery, i.e. the way bones repositioning affect the facial mimics of the patient, its mastication and speech production.

Finally, the sixth issue of the clinical protocol, namely the per-operative guiding, has been addressed by Bettega et al. (1996), Schramm et al. (2000) and Marmulla and Niederdellmann (1999) in a maxillofacial Computer Aided Surgery framework.

2.4 Our approach

Each step of the Computer-aided protocol for orthognathic surgical planning has been addressed by different groups. However, from our knowledge, none of these works completely addressed the whole protocol. Although the existing systems are very effective from a computer science point of view, they are gen-

erally irrelevant for clinical routine use because they do not take into account some of the essential clinical issues, namely the cephalometric and orthodontic analyses.

The first four steps of the computer-assisted protocol were addressed by our group (Bettega et al., 2000). A simulator was developed integrating a 3D reconstruction of the patient skull, a 3D extension of the 2D Delaire cephalometry (Delaire, 1978), and an orthodontic planning carried out on teeth plaster casts while tracked with an optical localizer. This simulator for diagnosis and planning of bone repositioning was validated on a dry skull. Some results on the transfer to the operating theater were proposed in Bettega et al. (1996, 2000), but clinical validation is not available yet.

The next parts of this paper focus on the fifth step of the protocol, namely the modeling of the soft tissue deformations resulting from bones repositioning.

3 Modeling of the patient face soft tissues

Once the surgeon has defined a bone repositioning planning, based on cephalometric and orthodontic criteria, the next step concerns the evaluation of the consequences of this planning on the facial soft tissues. A very important point is to predict the aesthetic face appearance after surgery. Another issue consists in evaluating the functional consequences of the intervention, in terms of facial mimics, mastication and speech production. This point, not addressed so far in the literature, is very challenging and requires an accurate modeling of the facial muscular structures.

To address these two issues, an accurate biomechanical face model integrating muscles must be defined for each patient. Before introducing our methodology, a study of face anatomy is presented to better apprehend the modeling requirements and difficulties.

3.1 Face anatomy

3.1.1 Anatomical and functional description

Facial tissues are composed of a complex interweaving of muscular fibers, fat, glands and mucosa (Rouvière and Delmas, 1997). The facial skin structure is basically made of three layers: the epidermis, the dermis and the hypodermis. The epidermis is a superficial 0.1 mm thick layer, mainly composed of dead cells. The underlying dermis layer, which is much thicker (0.5 mm to 4 mm), is composed of elastin fibers mainly responsible for the global elastic behavior
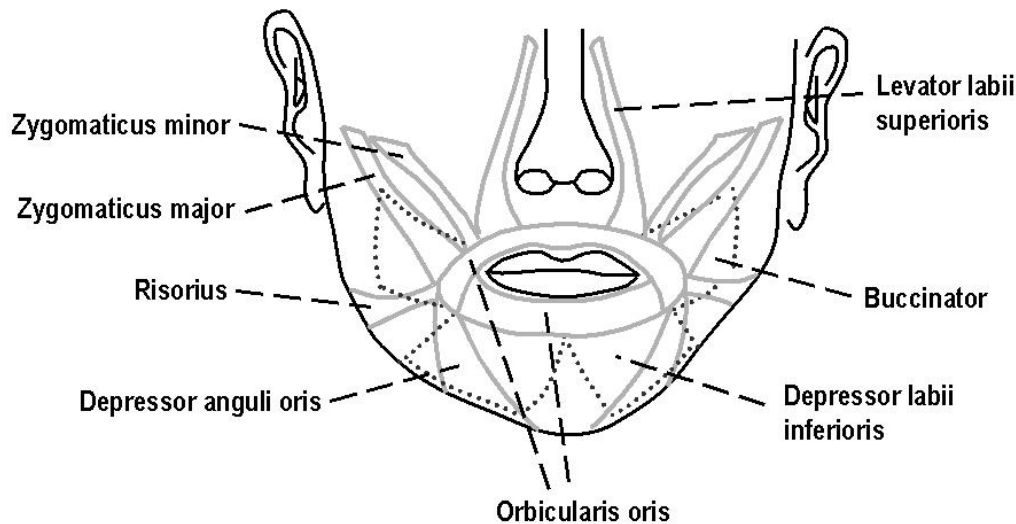
Fig. 1. Main muscles acting on the lips. The Orbicularis oris is a constrictor muscle, with fibers running around the lips. Others muscles are dilatators, with an insertion on the skull and one on the Orbicularis oris.

of the skin. Finally, the hypodermis layer, mainly fat tissues and mucosa, can slightly slide around over the bones of the skull and jaw.

The muscular structure that connects these skin layers to the skull is extremely complex, with insertion points, orientations and fibers interweaving allowing a great facial dexterity (mimics, expressions, lips gesture for speech production). As orthognathic surgery mainly affects the lower part of the face, i.e. the maxilla and the mandible, only the muscles inserted on these bone structures and their connections to the soft tissues surrounding the lips are described.

More than ten muscles play a role in the deformation of lips tissues, most of them being bilaterally symmetrical pairs of muscles (figure 1). The Orbicularis oris is a specific constrictor muscle, with fibers running around the lips. Its activation closes the lips and implies a protrusion gesture (forward movement of the lips). The other muscles that act on lips shape are dilators, with a distended action similar to the skeletal muscles action. These muscles are all gathered around the lips, with the same kind of insertions: one on the skull and the other on the Orbicularis oris muscle. Figure 2 plots the main directions of deformations for the production of facial expressions (Hardcastle, 1976). Deformations of the region surrounding the lips are essential for smile, sadness and speech production.

3.1.2 Mechanical properties

The biomechanical properties of skin tissues are difficult to characterize. As a first approximation, facial tissues can be considered as quasi-incompressible,
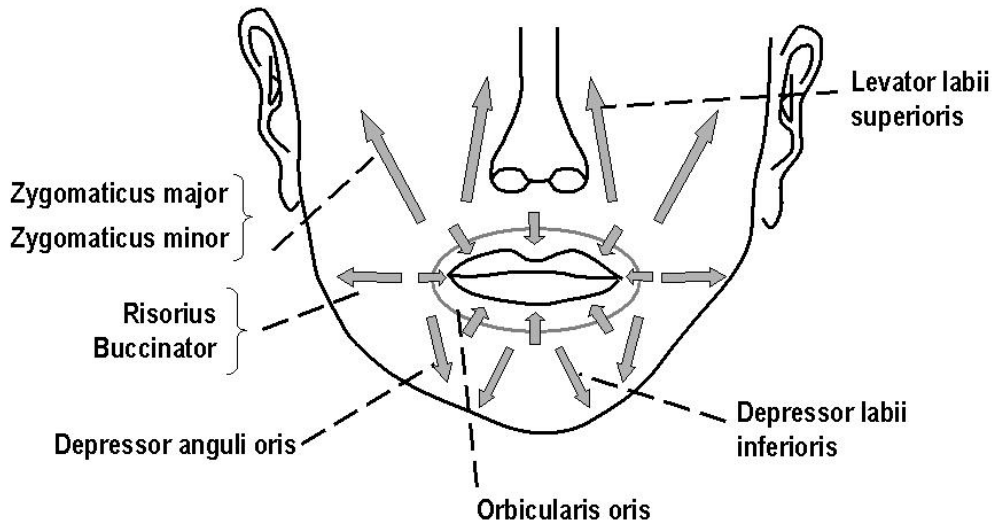
Fig. 2. Main directions of deformation that are important for the production of facial expressions (Hardcastle, 1976).

as they are mainly composed of water (Fung, 1993). Concerning skin stiffness, few studies present stress/strain measurements. Fung (1993) reports a complex relationship between stress and strain, summarized as a linear relationship if the strain ratio is below 15%, followed by an exponential-like behavior for larger deformations. The origin of this non-linear behavior can be found in the individual mechanical properties of skin tissues. Whereas the elastin fibers, in the epidermis and dermis, have a quite linear stress/strain relationship, the collagen has a highly non-linear stress/strain relationship, due to its visco-elastic behavior. Therefore, the collagen proteins seem to be responsible of the non-linear relationship experimentally measured for large deformations of the skin.

Concerning muscles, their main components are actin proteins, which have a linear stress/strain relationship. Facial muscles are also fiber-reinforced, contrary to passive skin tissues that have an isotropic behavior. Thus, mechanical properties are different in the direction of the fibers and in orthogonal directions. Moreover, it is reported that stiffness in the fibers directions increases with muscle contraction, while stiffness in transversal directions remains constant (Duck, 1990; Ohayon et al., 1999).

3.2   Finite Element Method to model soft tissue biomechanics

The most used method to describe the continuous mechanical behavior of soft tissues is the Finite Element Method (Zienkiewicz and Taylor, 1989). This method is based on a volumetric discretization of the structure, with the def-

inition of a 3D mesh. This mesh is made of small volumes, the *elements*, connected by *nodes*, the vertices of these elements. For 3D modeling, the most commonly used elements are hexahedrons, tetrahedrons, and wedges. The element type and the geometry of the mesh are essential from a numerical and mechanical point of view. Hexahedrons are preferred to tetrahedrons in terms of convergence, error estimation and computation time (Zienkiewicz and Taylor, 1989; Craveur, 1996; Ansys, 1999). Moreover, the size of the elements has to be adapted to the shape of the structure: more elements are needed in regions with a high surface curvature.

Two methods are classically used to define a Finite Element mesh, manually or with automatic mesh generators. Manually building a mesh is the optimal method as one can easily use hexahedral elements and control their distribution over the mesh. However this method is usually limited to one specimen due to the prohibitive amount of manual labor required to build the mesh. Therefore, automatic mesh generators have been developed to overcome this limit. Given the contour surfaces of an object, a volumetric unstructured mesh of tetrahedrons is automatically built. However, for very complex shapes, the generated mesh can present singular regions, i.e. with an extremely high density of elements. Besides increasing the number of degrees of freedom (hence the computation time), these singular regions can lead to artificial anisotropy inside the mesh and over-stressed areas (Craveur, 1996; Ansys, 1999).

3.3 Methodology

In the framework of computer-assisted facial surgery, a model of each patient is required. A 3D mesh adapted to each patient morphology must therefore be defined. Hence, existing Finite Element face models (Keeve et al., 1998; Roth et al., 1998; Schutyser et al., 2000; Zachow et al., 2000) are built from patient CT images using automatic meshing methods. However, these method usually lack robustness because of the complex geometry and topology of the face soft tissues, and the computing time is generally several hours, which is not compatible with a clinical use. In addition to the computation drawbacks inherent to automatically generated meshes, these models are limited in terms of biomechanical modeling. Indeed, the unstructured organization of the elements does not allow to identify one anatomical structure from another within the mesh. The face soft tissues are thus modeled as a single entity, without distinctions between dermis layers, fat, muscles and mucosa. This results in considering the model as isotropic, without taking into account the specific mechanical properties of each tissue and therefore the resulting anisotropy. Moreover, because of the unstructured organization of the elements, muscles cannot be easily modeled within the mesh, and the functional consequences of the bones repositioning are therefore not evaluated.

The methodology presented in this paper has been defined to overcome some of the shortcomings of these existing models. It consists, first, in manually defining a structured 3D mesh, in order to build one generic model of the face. Emphasis is given on the design of the generic mesh, so that the elements inside the mesh can be associated to anatomical entities (dermis layers, fat, muscles, mucosa...). Specific mechanical properties can therefore be explicitly set to fiber-reinforced muscles (described as transverse isotropic structures), while other tissues are considered isotropic. Moreover, as the type and size of the elements is controlled during the mesh design, the numerical limits of automatically generated meshes are avoided. However, such a manual elaboration of the model is extremely complex, long and tedious, hence cannot be considered for each patient in a clinical planning. Therefore, the next step of our methodology consists in conforming the generic model to each patient morphology, using an automatic registration method: a structured Finite Element model of each patient is then automatically generated. This conformation process is presented in section 3.5.

3.4 A generic 3D biomechanical model of the face

3.4.1 3D mesh construction

In the framework of the Finite Element Method, a 3D mesh of a generic human face was developed. It is divided in small volumes, the *elements*, which are connected by *nodes*, the vertices of these elements. Our goal was to build a mesh of the facial soft tissues that enables to specify separate anatomical structures, different muscles and fat. The idea was then to label elements of the mesh with respect to the component they belong to. This element-labeling task is difficult to achieve in an unstructured tetrahedral mesh, such as the ones automatically generated from CT exams. Therefore, we manually designed a structured mesh that represents a generic face. It is composed of regular hexahedral and wedge elements. Some of these elements are used to model the main muscles, while others represent mucosa and fat tissues. This mesh is finer in regions where more accuracy is required, such as the lips and mouth, and coarser elsewhere.

As a starting point, a 3D surfacic mesh, developed for computer animation (Guiard-Marigny et al., 1996), was manually redesigned to take into account facial muscles courses. This mesh, which represents the "external" surface of the skin, was used to create two other surfaces. The "internal" surface models the inner boundary of soft tissues, that lays on the skull, while the "intermediate" surface is at the interface between the dermis and the hypodermis. Finally, two layers of hexahedral and prism elements were defined by connecting nodes of these surfaces (figure 3). The outer layer of elements represents
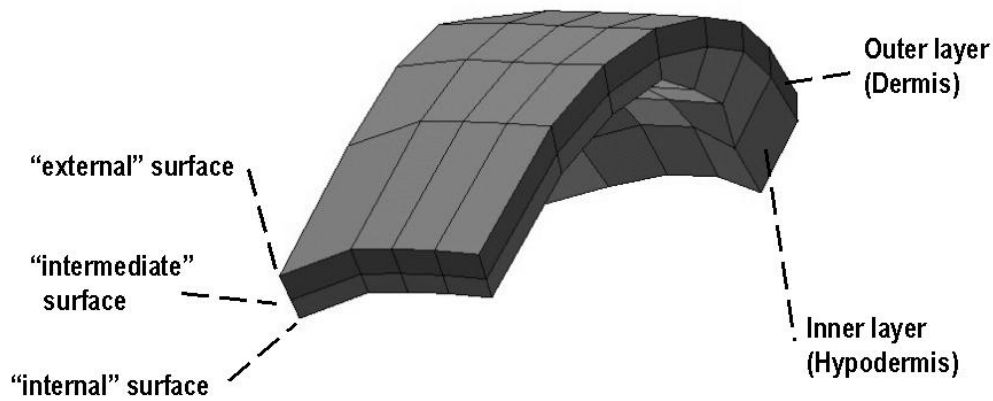
Fig. 3. Nodes of the mesh form three surfaces: the "internal", "intermediate" and "external" surfaces. Two layers of elements are defined by connecting nodes of these surfaces. The outer layer represents the dermis tissues, while the inner layer models the hypodermis tissues.
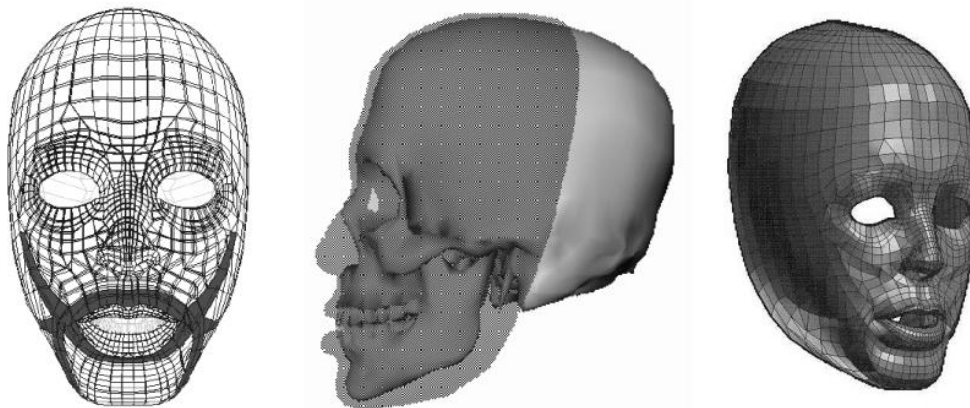

Fig. 4. Several views of the generic 3D mesh (with the lips open). Muscles included in the mesh are highlighted in the frontal view.

the dermis tissues, while the inner layer models the hypodermis tissues. Both layers have a non-constant thickness since the dermis and hypodermis are not homogeneously thick. As a first approximation, the very thin epidermis layer is not included in the current mesh. Figure 4 shows several views of the 3D generic mesh of the face, defined by 2884 elements and 4215 nodes.

In order to identify facial muscles, elements located along the course of muscles were labeled, to set specific mechanical properties and to simulate muscular activation. The main facial muscles surrounding the lips were integrated. These muscles being rather superficial, they were included in the outer layer of the mesh. Because they are not directly responsible for lip movements, strong mastication muscles attached to the mandible are not modeled in the current

version of the model.

In order to simplify the model, facial muscles were grouped with respect to their action on the lips (figures 1 and 2; Hardcastle (1976)). Therefore, muscles with similar action are represented in the mesh within a single muscle structure. For example, Buccinator and Risorius muscles are modeled together, as they have roughly the same function of retracting the corners of the mouth. Muscle structures currently included in the model (Orbicularis oris, Zygomaticus major and minor, Buccinator and Risorius, and Depressor anguli oris muscles) are shown in figure 4. Levators and Depressors muscles are not yet modeled but will be added later. As can be noticed in figure 4, the lips of the generic model are opened. In order to facilitate the conformation of the model to patient whose lips were closed during the CT exam, a second version of the generic model was elaborated with the lips closed.

3.4.2 Mechanical parameters

In order to restrict the modeling complexity and time computation, a linear elastic behavior was assumed for facial tissues (this limitation is discussed in section 6.3). Due to this linear assumption, our model is not correct for relative strains that run after 15%. However non-homogeneity and anisotropy of face tissues are partly taken into account, as fiber-reinforced muscles are included in the model.

Under linear elastic assumptions, mechanical properties are determined by two parameters, the Young modulus E and the Poisson ratio ν (Zienkiewicz and Taylor, 1989). The Young modulus corresponds to the stiffness of the material, that is to say the way it responds to external pressure forces. For linear elasticity assumption, E is approximated by the slope (at the origin) of the measured stress/strain relationship. The Poisson ratio measures the way a deformation in a given direction can induce deformations in orthogonal directions. This elastic parameter is indirectly linked to the compressibility of the structure: a value close to 0.5 describes a quasi-incompressibility of the material.

Two kinds of Finite Element structures are defined, with two different sets of mechanical characteristics. The first set defines the behavior of most of the elements, associated to "inactive" tissues (skin, mucosa and fat). According to Fung (1993) measurements, a Young modulus value of 15 kPa was used for these tissues. Skin tissues, mainly composed of water, are considered quasi-incompressible. The Poisson's ratio ν was therefore set to 0.49 (a value of 0.5 is inadequate for numerical constraints). Muscular fibers, located along the course of facial muscles, are characterized by the second set of properties. The muscular fibers behaviors and measurements reported by Duck (1990)
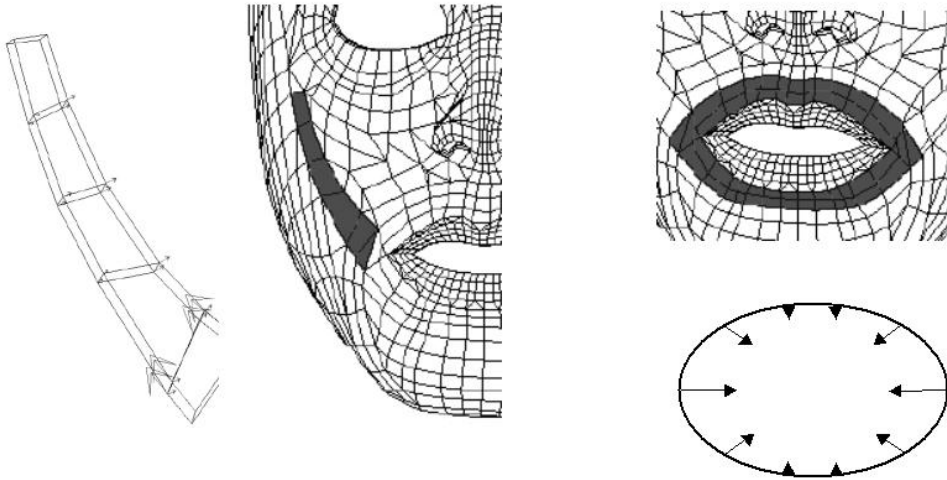
Fig. 5. Level of forces generated for two muscles. Left, a classical skeletal muscle, the Zygomaticus major. Right, the Orbicularis oris muscle, with a sphincter action.

are used for the mechanical characteristics of these "active" elements. Each element labeled as "active" is modeled with a transverse isotropic stress/strain relationship. This assumption requires two parameters for stiffness: a Young modulus E_{fibers} in the main fibers direction, and another modulus E_{ortho} in orthogonal directions. Following Duck (1990) measurements, a stiffness value of 6.2 kPa is used for both Young modulus at rest, while E_{fibers} is set to 110 kPa when muscle activation is maximum. Therefore, E_{fibers} values linearly increase with muscular activation, while E_{ortho} value remains constant.

3.4.3   Force generation

A muscle is represented by a sequence of adjacent elements inside the outer layer of the 3D mesh (figure 4). Muscular contraction is modeled by a low-level force generator applying forces on the nodes of this sequence of elements. The generated forces are mostly concentrated at the two muscle extremities, in the main fibers direction. They tend to shorten the muscle under activation. Facial muscles directions being not straight but often curved, a distributed model of force is applied on nodes located between the two extremities of the muscle. This distributed model adds, on each node between extremities, forces that are function of the muscle curvature, and tends to straighten the muscle during activation. Figure 5 plots the forces generated for two muscles: a classical skeletal muscle, the Zygomaticus major, and the constrictor Orbicularis oris muscle. Note the influence of the force-distributed model on the Orbicularis oris muscle: directions of action tend here to shorten the constriction to give a circular shape to the lips.
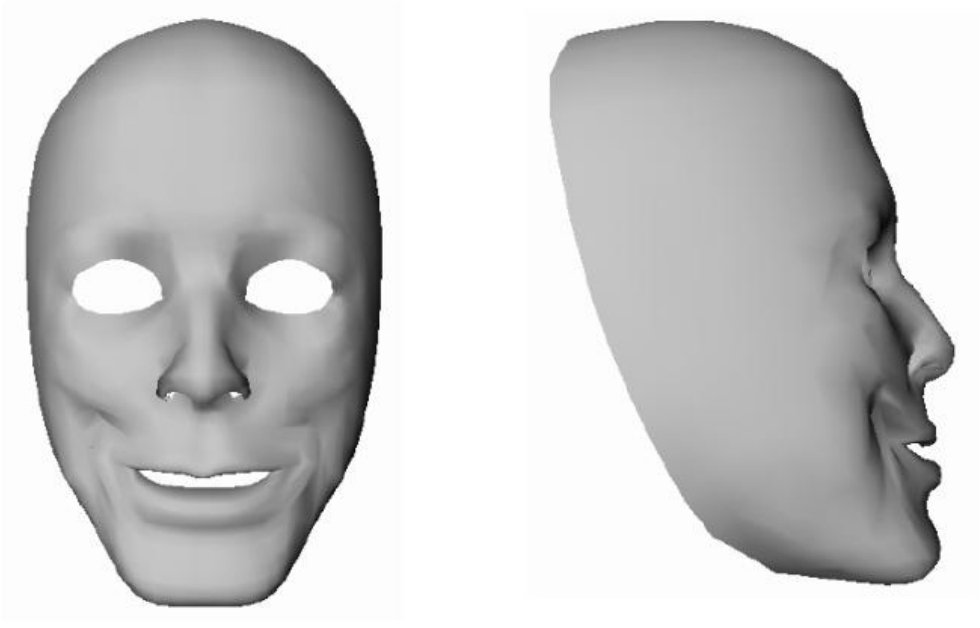
Fig. 6. Face deformations due to the activation of the two symmetrical parts of the Zygomaticus muscles.

3.4.4 Boundary conditions

Although the hypodermis tissues can slightly slide around over the bones of the skull and the jaw, it is assumed that these tissues are rigidly fixed to the bones. Therefore, constraints with no-displacement are added to nodes of the "internal" surface of the mesh. Note that only the nodes that are supposed to be in contact with the skull and the jaw are fixed, while the nodes located in the cheeks and lips area are left free to move.

3.4.5 Simulated deformations under muscles contractions

Simulations were carried out with two Finite Element packages, either Castem™or Ansys™, with a quasi-static resolution algorithm. The low-level force generator described above was applied on each muscle structure. Figure 6 shows the facial deformations due to the activation of the two symmetrical parts of the Zygomaticus muscles, with a force intensity of 1 Newton. These muscles are partly responsible for the smile gesture, and the simulations plotted in figure 6 seem coherent with this behavior.

Figure 7 plots two other facial expressions due to individual muscular contractions of the Depressor anguli oris muscles, which is partly recruited in a "sadness" gesture (top), and the consequences of the Orbicularis oris muscle activation (bottom). Note that the Orbicularis oris contraction induces a lips constriction (what seems coherent with the sphincter action of this muscle),
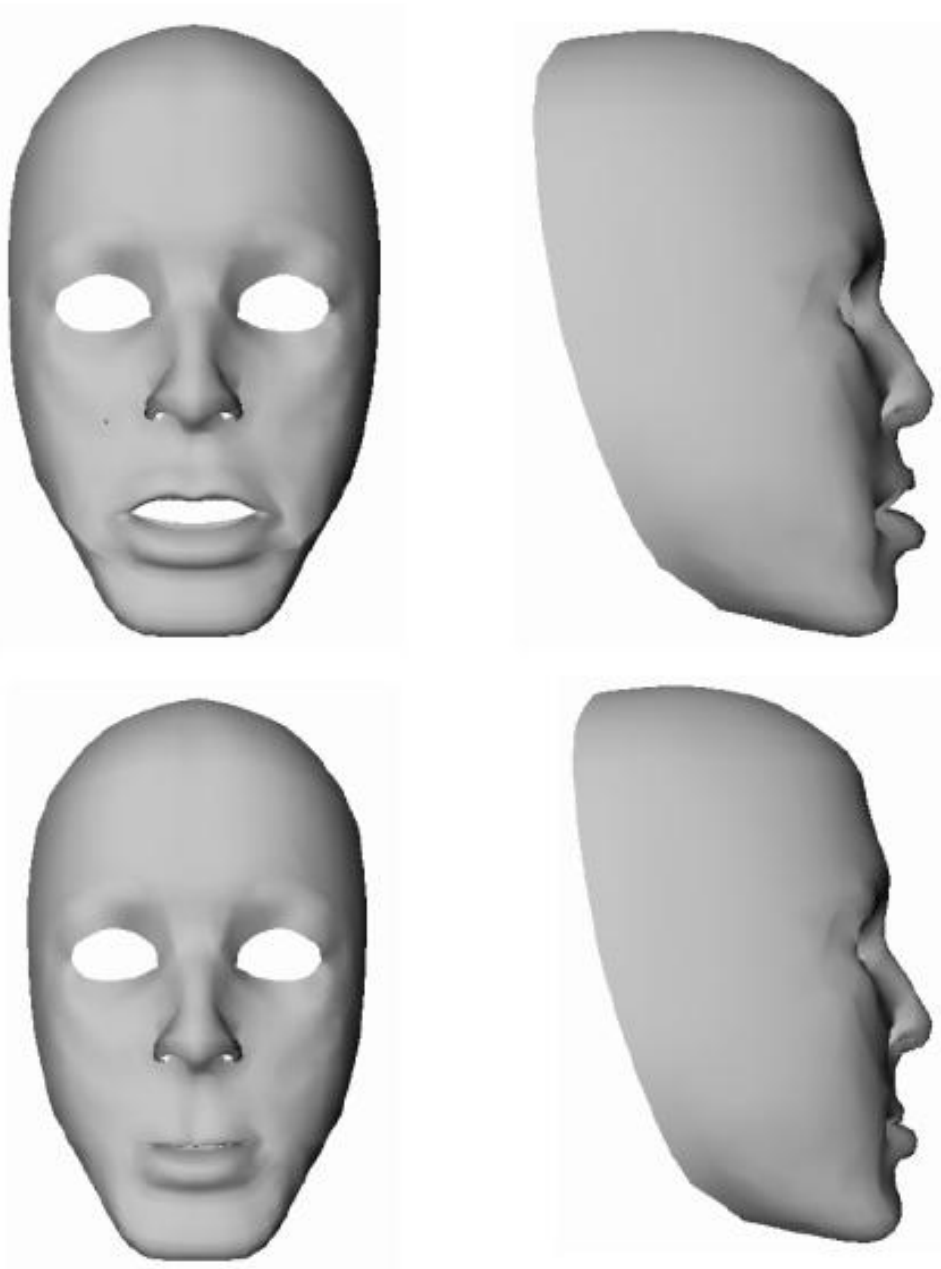
14

Fig. 7. Action of Depressor anguli oris muscles (top). Activation of the Orbicularis oris muscle (bottom): the inward movement of the lips inside the mouth is due to the absence, in the modeling, of any lips/teeth contact.

and an inward movement of the lips. We assume that the latter unrealistic movement is mainly due to the absence, in the modeling, of any lips/teeth collision detection and contact.

Although these simulations are coherent with real face movements, their realism could be greatly improved by contracting several muscles simultaneously.

15

Indeed, face movements always result form the activation of several muscles; a single muscle never contracts alone. Hence, this requires a complex motor control handling, which is a very tough problem (Hardcastle, 1976).

3.4.6   Simulation of bone repositioning

While forces are used to simulate muscles contraction, different loads must be applied in the case of maxillofacial surgery. To simulate the planned bone repositioning, internal nodes of the mesh that are in contact with the mobilized bone segments (maxilla and/or mandible) are displaced according to the surgical planning. Other nodes in contact with the skull are fixed, and nodes in the mouth area are unconstrained.

3.5   Conformation of the generic model to the patient face morphology

3.5.1   Principle

Usually, Finite Element analyses are limited to only one specific case due to the prohibitive amount of manual work required to generate a 3D mesh. This is particularly the case for meshes of living tissue, which can be tough to generate automatically because of their very complex geometry. Powerful models are available, but are not appropriate to clinical applications: they usually represent atlases that are not specifically adapted to each patient.

For that reason, some authors working in the field of computer aided craniofacial surgery or face animation have proposed to adapt generic models to individual patient anatomy (see for example Lee et al., 1995; Barré et al., 2000; Mao et al., 2000). Feature-based correspondence techniques are generally used, which require the interactive manual definition of landmarks on patient data. Although these methods have been successfully applied to geometric surfaces or 3D mass-springs models, their application to volumetric Finite Element models is not straightforward. Indeed, the shape of each element of a mesh must fulfill strong regularity constraints to enable Finite Element computations (c.f. section 3.5.4.1). Existing methods enable to conform generic meshes to individuals using exclusively geometric criteria, without ensuring the mesh regularity is conserved. Hence, there is no guaranty that resulting models can still be used to perform Finite Element analysis.

Our research team has proposed a completely automatic approach, the Mesh-Matching method, to generate patient specific models (Couteau et al., 2000). Assuming a generic model (3D mesh + biomechanical properties) is available, it can be automatically adapted to patient data, CT scans in Couteau et al. (2000), by the mean of elastic registration. Although the Mesh-Matching al-

gorithm was successfully validated on 15 femurs (Luboz et al., 2001a), the patient face meshes generated using this method for maxillofacial application could not be directly used for Finite Element simulation. Indeed, the mesh regularity was not preserved during the conformation to patient morphology. Therefore, a post-treatment algorithm was added to automatically detect and correct mesh distortions, in order to carry out Finite Element analysis. This correction algorithm is introduced in section 3.5.4.2.

3.5.2 Patient data

Different kind of data can be collected before orthognathic surgery. Two teleradiographies (sagittal and coronal) of the patient head plus a dental orthopantomogram are systematically acquired, while MRI and/or CT exams are more rarely used. Although we are conscious it is limitative, a CT exam of the patient face is required, with a region of interest between the tip of the chin and the eyes. Indeed, this kind of data was already used in our team by Bettega et al. (2000) to build a diagnosis for osteotomies, integrating cephalometric and orthodontic criteria. Also, the invasivity of the scanner, despite being more important than the teleradiographie's one, is drastically reduced with new-generation multi-slices machine.

Both skin and skull surfaces are built out of CT images, using the Marching-Cubes algorithm (Lorensen, 1987). These surfaces are primarily used for 3D visualization and to establish the cephalometric analysis. However, these surfaces cannot be directly used to conform the generic model. The Marching-Cubes algorithm reconstructs isosurfaces inside a 3D volume, including internal structures of the skin and skull (sinus, internal bones, etc). Only the external surfaces of the skull (respectively the skin) are necessary to conform the generic model to the patient morphology. Hence, a ray-tracing algorithm is used to extract visible points of the 3D isosurfaces, i.e. two clouds of 3D points lying exclusively in the skin and the external surface of the skull.

3.5.3 Mesh adaptation

After the segmentation step, the generic mesh is deformed so that it fits the patient skin and skull surfaces, using the *Octree Spline* elastic registration method (Szeliski and Lavallee, 1996). This algorithm computes a deformation function T that matches two surfaces together, with both surfaces represented as a cloud of 3D points. This elastic transformation T is a combination of a rigid transformation, a global warping, and local deformations functions. The parameters of T are evaluated by optimizing a disparity function based on the distance between the two surfaces.

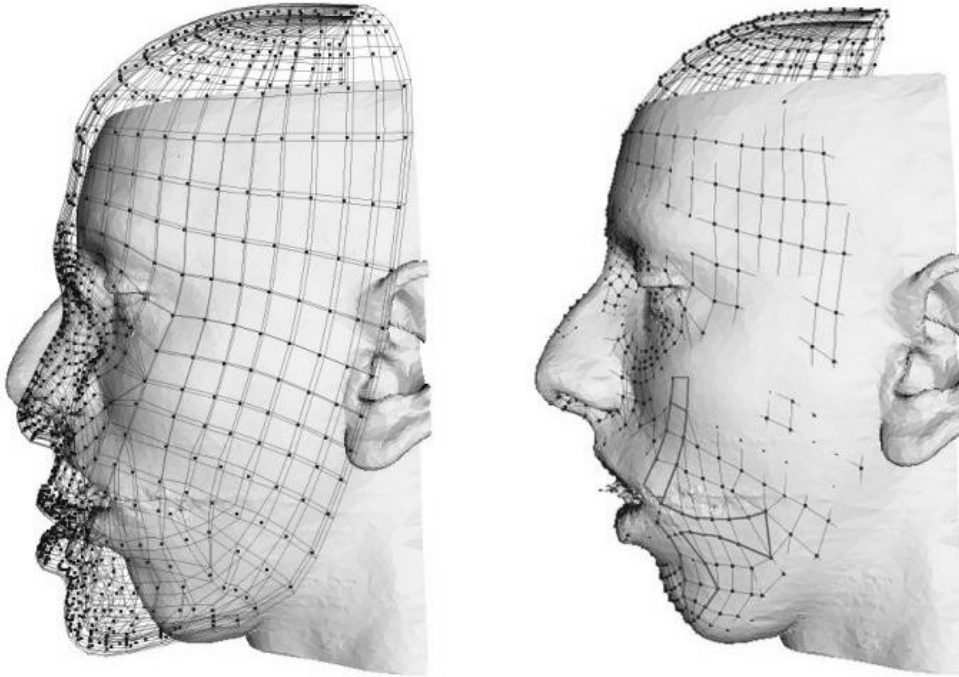The 3D mesh of the patient is generated in two steps:

Fig. 8. An elastic transformation T_{ext} is calculated to match nodes of the "external" surface of the generic mesh to the patient skin surface. The mesh is rendered in wire frame while the blue points represent the displaced nodes. In the image after registration (right), the elements representing muscles of the model are highlighted to show the inferred location of the patient muscle on the face.

(1) A first elastic transformation T_{ext} is calculated to match nodes of the "external" surface of the generic mesh to the patient skin surface. This transformation is then applied to all the other nodes of the mesh. Figure 8 illustrates this first registration step. An animation showing the actual matching procedure between the two clouds of 3D points representing the patient skin and the outer nodes of the generic mesh is available on the publisher electronic annexes web site.

(2) A second elastic transformation T_{int} is afterwards computed to match nodes of the "internal" surface of the mesh to the patient skull surface (figure 9). Actually, only nodes that are physically in contact with the skull are considered for this transformation while nodes located in the area of the nose are not modified.

3.5.4 Mesh correction

This new patient mesh being generated for Finite Element computation, the shape of each element must fulfill regularity criterion.
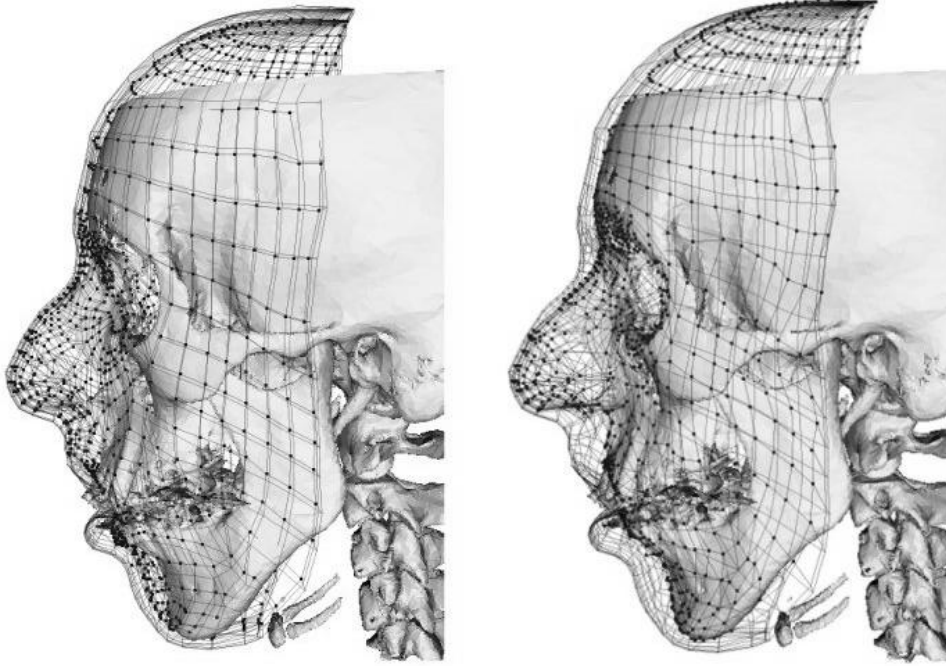
Fig. 9. Transformation T_{int} is calculated to match nodes of the "internal" surface of the mesh (blue points) to the patient skull surface. Only nodes attached to the skull are transformed. Nodes that belong to the lips, cheeks and cartilage of the nose are not moved.

3.5.4.1 Element regularity for Finite Element formulation In the framework of the Finite Element method, linear elasticity equations are globally solved over the domain as a summation of numerical integration on each element of the mesh. In order to simplify this integration, a reference element with a regular shape is defined in a natural coordinate system (Touzot and Dhatt, 1976; Zienkiewicz and Taylor, 1989), i.e. with coordinates (r, s, t) running from -1 to +1 (or 0 to 1). For each element of the mesh, numerical integration is performed in the reference element, then transferred to the actual element using a polynomial shape function τ that maps natural coordinates (r, s, t) to the actual coordinates of the element (x, y, z) (figure 10).

The shape of an element e is considered as "irregular" if it is not possible to define a function τ that maps the reference element to e. Mathematically, that happens when the jacobian matrix J of the shape function τ is singular, that is to say when $\Delta(J)$, the determinant of J, is equal to zero. The value of $\Delta(J)$ inside the element is calculated by interpolation between its values on each node of the element. Hence, it is never null if its values on each node have the same sign and are not equal to zero. Therefore, the condition for "regularity" is that $\Delta(J)$ remains strictly positive (by convention) on each node of the element.
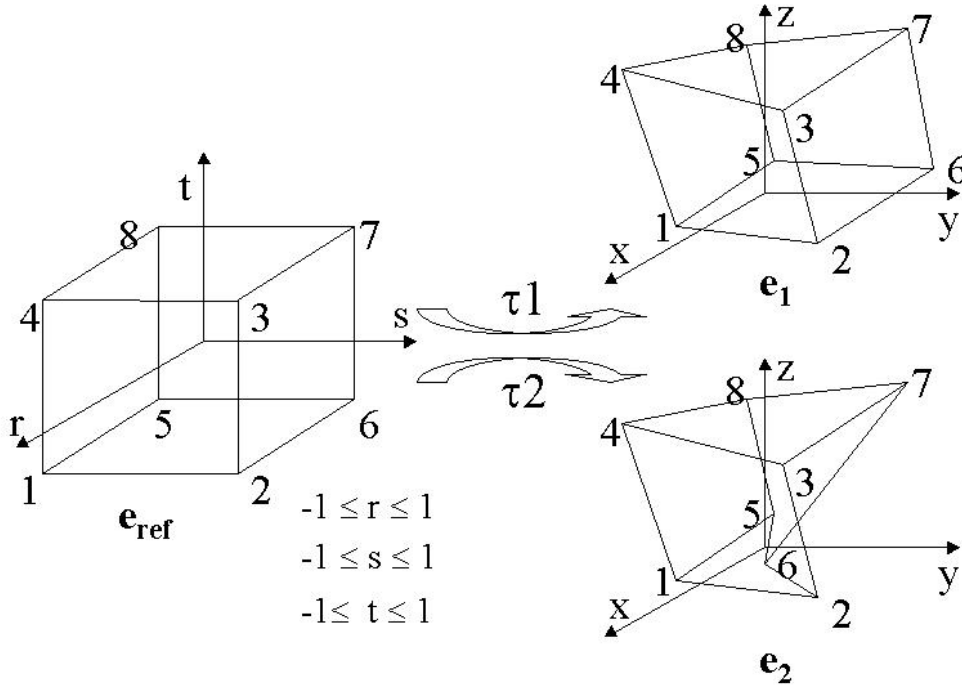
19

Fig. 10. Shape function τ_1 maps natural coordinates (r, s, t) to the actual coordinates (x, y, z) of element e_1. Shape function τ_2 cannot be calculated due to distortions of element e_2.

Although it cannot be seen in the patient meshes represented in figure 11, every model had elements detected as "irregular" (see section 5.1.4). To correct these irregularities, a post-treatment must be performed after the initial M-M algorithm.

3.5.4.2 Correction of distorted elements Geometrically correcting a set of elements inside a 3D mesh is a complex, ill-posed problem without any straightforward solution (Cannan et al., 1993; Freitag and Plassmann, 1999). Indeed, correcting a single element can distort its neighbors while they were originally regular. All elements must therefore be corrected altogether.

The proposed correction algorithm consists in an iterative process: nodes of irregular elements are slightly moved at each step, until every element is regular. An iteration consists in:

(1) Computing $\Delta(J)$ for each element of the mesh.
(2) Detecting irregular elements ($\Delta(J)$ negative on some nodes of the element).
(3) Correcting each irregular element. For this, nodes with negative $\Delta(J)$ values are moved in the direction of the gradient of $\Delta(J)$, which is analytically computed. Displacements are pondered by the absolute values of

20

$\Delta(J)$. Displacement vectors of nodes shared by several irregular elements are the summation of displacement vectors computed for each element.

In addition, maximal nodes displacements are constrained so that the corrected mesh still fits the patient morphology. For the face application, distance between the initial and final position of nodes cannot exceed 1mm for nodes of the "external" surface, and 3mm for the other nodes.

This algorithm corrects irregularities of the elements, which is necessary to resolve the Finite Element method computations. Another issue concerns the quality of the elements (aspect ratio, warping factor, parallel deviation, etc.), which directly influence the precision of the simulations. Although improving the elements quality concerns future works, first results are presented in Luboz et al. (2001b).

4 Clinical validation protocol

An important issue is to evaluate the quality of the presented method, from a clinical point of view. Both the adequation of the model to the patient morphology and the simulation of the post-operative aspect must be validated.

4.1 Evaluation of the mesh conformation

The first point to evaluate is how well the patient model matches the actual patient morphology. To assess the importance of the location of the maximal errors and the way it affects the perception of the model, a qualitative evaluation was carried out. Six patient models (see results in section 5.1) were submitted to five maxillofacial surgeons of the Plastic and Maxillofacial department of Purpan Hospital, Toulouse, France. They could examine each model with an interactive 3D visualization and with facial, lateral and profile printouts. Surgeons were asked about their perception of the morphological similarities and differences between the patient models and the patient's skin surfaces reconstructed from the CT exams (figure 11).

4.2 Qualitative validation of the simulations

A second point consists in evaluating the prediction of the patient postoperative aspect. For a quantitative validation, post-operative data are required. Unfortunately, these data are not available so far. The patients used to

test our method have not all been operated yet, as they pursue an orthodontic treatment preceding the surgical intervention. Moreover, a period of six months to a year must be respected before the acquisition of post-operative data, to enable healing and stabilization following the surgery.

A qualitative validation was nevertheless performed. The five surgeons were asked how well they think the simulations matches what they would be expecting, with respect to the patient dysmorphosis, the surgical planning and their clinical experience.

5   Results

Six patient models generated with the method described in this paper are presented. Then, simulations of soft tissue deformations resulting from bones displacements planned for two patients are provided. In both case, a qualitative analysis of specialized surgeons is presented.

5.1   Patient models

5.1.1   Mesh conformation

First results concern the generation of patient specific Finite Element models. Pre-operative CT exams of six patients were provided by the Plastic and Maxillofacial Department of Professor F. Boutault in Purpan Hospital, Toulouse, France. Figure 11 shows the six patient models built with our method, with the skin and skull surfaces segmented in the patient CT images. Depending on the patients lips posture during CT acquisition (closed or opened), the generic model with lips closed or the other one with lips opened was used for the conformation. Patient models were successfully generated despite the large diversity of morphologies. The incorrect appearance of the models eyes is due to the different topology between the generic model (which has two "holes" in place of the eyes) and the skin surfaces.

5.1.2   Model accuracy

The root mean square error of the registration algorithm was between 0.3 and 0.55 mm for every model. Hence, the precision is around 1mm considering the marching cubes error. Also this registration error seems numerically quite satisfying, the distances between the model nodes and the patient skin surface reconstructed from the CT exam are not homogeneously spread out over the mesh. The maximal errors are located in some specified areas. For example,
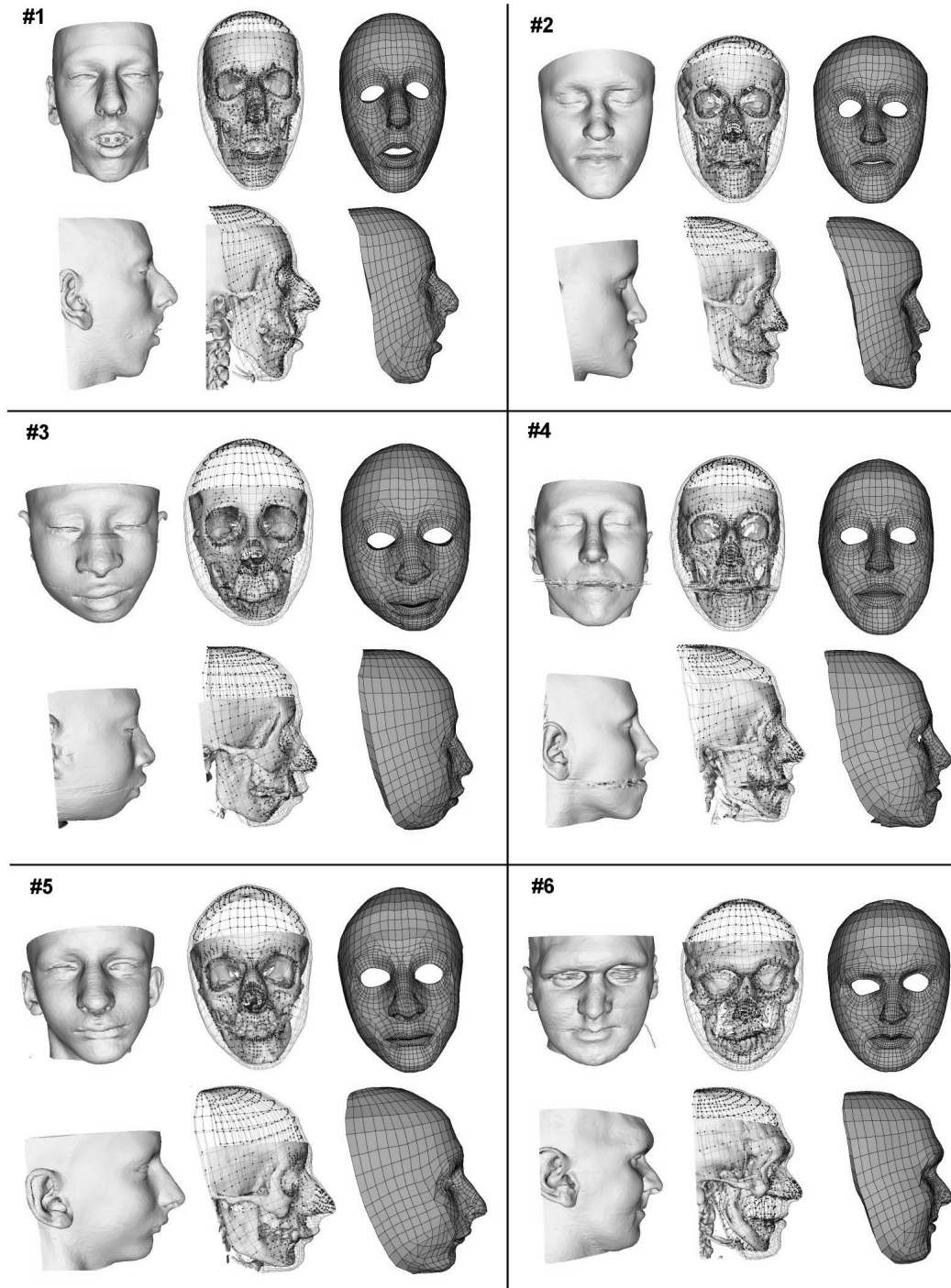
Fig. 11. Six automatically generated patient face models. For each model, the left tiles represent the skin surface segmented from the CT images and reconstructed using the Marching Cubes algorithm. The central tiles show the skull surface and the mesh in wireframe. The inner nodes of the mesh are also visible so that their position with respect to the skull can be evaluated. Finally, the right tiles represent the patient model. The repartition of the elements is globally conserved, and muscle structures are still visibles.

23

the posterior border of the mesh does not fit the patients morphology well. Usually, this does not affect the areas that are relevant for orthognatic surgery. However, some models present important errors in the nose and lips area.

To evaluate the importance of the location of the maximal errors and the way it affects the perception of the model, the qualitative evaluation described in section 4.1 was realized. Five surgeons were asked how well the patient models match the actual patients morphologies, without knowledge of the numerical results evaluating the registration accuracy. At a first glance, most of the surgeons were disturbed by the lack of eyes and neck of the model. Although it may not be essential for our application, the overall aspect of the model is degraded. Overall, the clinicians point of view is that the shape of the model is similar to the patient morphology. However, important differences remains, mostly visible on the frontal view, which appearance is considered too flat. Nostril areas are regularly underestimated as well as cheekbones contours. Difference was made between small profile angles (called skeletal class III, as patient #2 and #4) and large ones (called skeletal class II, as patient #1, #3 and #5). For patient with small profile angle, nasolabial angle and maxillary and mandibular sulcus contours (around the lips) can be underestimated.

5.1.3 Robustness of the registration

As can be seen on the 3D reconstructed skull models, patients usually wear braces, as required by the orthodontic treatment preceding the surgery. These braces, as well as teeth fillings, can create artifacts in the CT images that are clearly visible in the 3D geometric models reconstructed using the Marching-Cubes algorithm. Although these artifacts decrease the quality of the skull and skin graphical representations, they do not affect the registration algorithm used to conform the generic model to patient morphology. For example, face model #4 in figure 11 was successfully built despite these fillings artifacts, without any manual intervention to clean the CT slices.

Case #6 is also interesting because this patient, suffering from a bone disease, had the maxilla removed in a previous intervention to prepare for bone transplant. In this particular example, the registration algorithm was unable to find a suitable position for the internal nodes of the mesh that should be located in the maxilla area. These nodes were therefore considered by the registration algorithm as outlayers, then not taken into account for the computation of the elastic transformation (see section 3.5.3). They were however moved by the final computed transformation: as can be seen in figure 11 (sagittal view of the model #6), the approximation of the upper lips depth is still relatively good considering the absence of data between the base of the nose and the teeth in the mandible.

Patient	#1	#2	#3	#4	#5	#6
Number of irregular elements	234	239	253	191	268	291
Number of iterations	350	390	402	290	340	320
Number of nodes displaced	866	882	834	769	918	979
Mean displacement (mm)	0.31	0.29	0.30	0.30	0.17	0.16
Max displacement (mm)	2.90	2.20	2.49	3.00	2.19	2.30

Table 1
Results of the mesh regularization algorithm. For each patient, this table indicates the number of irregular elements after the conformation step, the number of iterations to correct the mesh regularity, the number of nodes displaced and the mean and maximum displacements of these nodes. The displacements are bounded to 1mm for the outer and inner nodes, and 3mm for the nodes inside the mesh. The mesh has 4215 nodes and 2884 elements.

5.1.4 Regularity of the generated meshes

As shown previously, the matching process was validated in terms of adequation between the patient morphology and the generated face model. If one focuses on the arrangement of the elements inside the meshes, no observable mesh disruption is noticeable. However, every mesh presented geometric irregularities after the conformation, disabling their use for Finite Element computations. Hence, the correcting post-treatment algorithm introduced in section 3.5.4.2 was successfully applied to all models presented in figure 11. Table 1 provides the number of iterations and node displacements required to automatically correct the meshes. Computation times range from 2 to 7 minutes on a 500Mhz DEC Alpha workstation.

5.1.5 Evaluation of the muscle location on the patient models

As can be seen on the patient models, symmetry, size and arrangement of the elements inside the meshes are globally conserved, and structures labelled as muscles are still clearly identifiable (figure 8). Although no patient-specific information about muscles courses were considered to conform the models, muscles structures are still represented in the patient meshes. Muscles can therefore be integrated in each patient model, with their specific geometries and mechanical properties. Figure 12 shows for three patient models the insertion location of the left Zygomaticus muscle of the model on the Zygomaticus bone, compared to an anatomical reference. Although no accurate measurement of the error is currently possible, inference of the muscle location seems qualitatively validated.
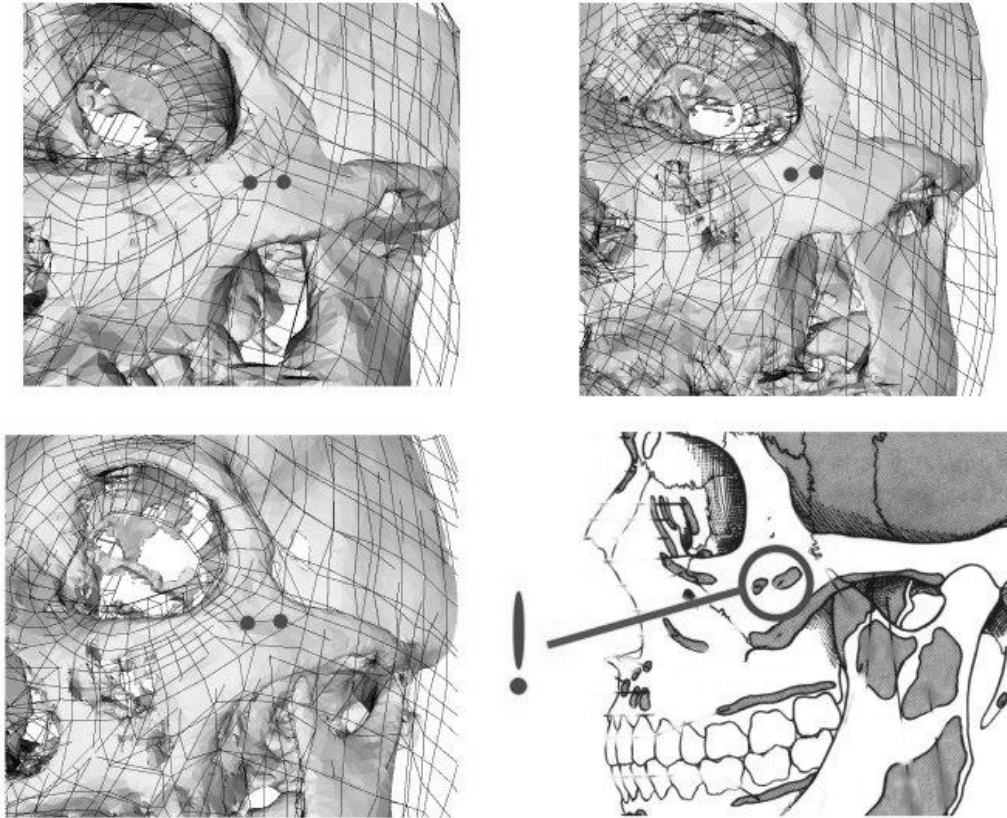
Fig. 12. Insertions of the left Zygomaticus in models #3, #1 and #4. The two points represent the nodes of the Zygomaticus elements that are rigidly fixed to model the muscle insertion. An anatomical reference in presented, showing the theoretical insertions of the Zygomaticus Major and Minor muscles in the bone.

5.1.6 Method use

While the different tasks to generate a model of a patient are fully automatic, models are built under close interactive control. The user can check after every step whether the results are satisfying or not, and restart the step with different parameters if required. The main points to check before conformation are the quality of the skin and skull 3D reconstruction and the initial position of the generic model compared to the patient skin surface segmented on the CT exam. This initial position is automatically computed by registration of both inertia referential. As the referential of the CT images can vary from device to device, it may happen that the generic model and the segmented skin and skull 3D surfaces are differently oriented. For the six models presented in the paper, the initial attitude had to be modified in two cases (patients #3 and #5). The generic model was too large for these two patients (two children) and then had to be manually scaled. Convenient tools are provided in the user interface to scale, translate and rotate 3D models.
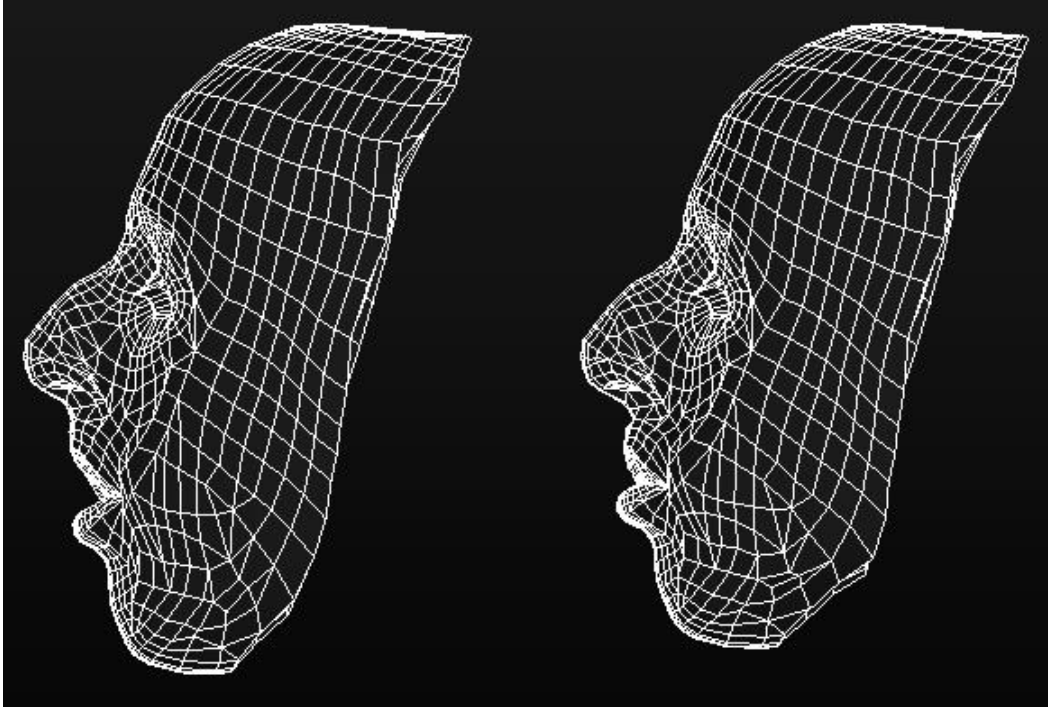
Fig. 13. Simulation of mandible and maxilla repositioning on patient #1.

The total building time for each presented models ranged from 15 to 35 minutes, mostly the computing time required to build the Marching-Cubes and to correct the mesh regularity. As the manual intervention time is limited, this model generation method seems suitable for a surgeon to be routinely used in a normal surgical planning setup. This is a strong improvement in comparison to automatic meshing algorithms, which usually require several hours of computation and manual intervention to correctly define the boundaries of the soft tissues to be meshed.

5.2   Simulation of bones displacements

Simulations of soft tissue deformations resulting from bones displacements were performed on two case studies, patients #1 and #2. The clinical diagnosis for patient #2 is to apply an 8mm backward displacement to the mandible. Procedure for patient #1 is more complex, as the upper maxillary must be moved backward from 2 to 3mm, while the mandible must be displaced upward and forward from 5mm and 8mm respectively.

Results presented in figures 13 and 14 were realized using Ansys™. No initial stresses or strains were considered for the models. As a starting point, facial tissues were assumed to have a linear mechanical stress/strain relationship, and relative deformations were supposed to be under 15%, which can be considered acceptable in a small deformation framework. As discussed at the end
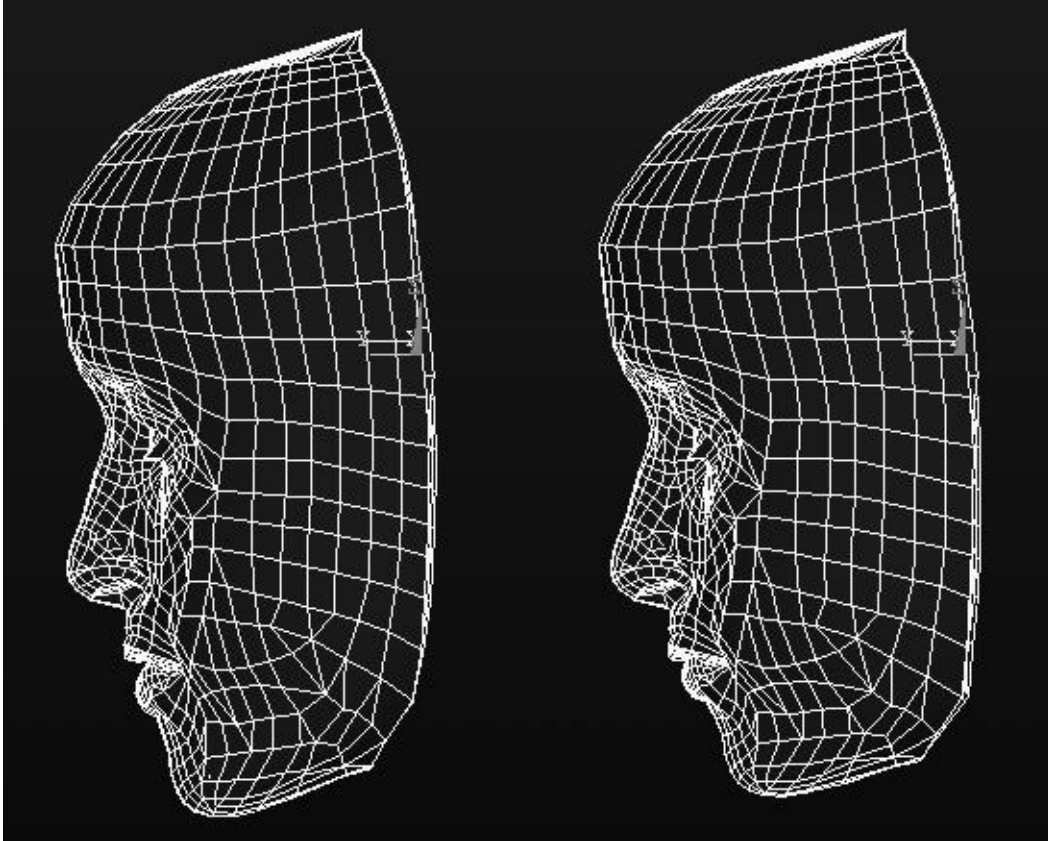
Fig. 14. Simulation of mandible repositioning on patient #2.

of this paper (section 6.3), these assumptions may be further reviewed through a more realistic modeling framework. Another point to improve realism of the simulations will be to acquire face texture for each patient and to apply it to the patient model.

As for the model adequation, a qualitative study was realized (see section 4.2). Surgeons were asked how well they think the simulations matches what they would be expecting. Their conclusions are that the modifications observed on the simulations are morphologically coherent, i.e. similar to what is clinically observed. The main changes are antero-posterior (as seen on sagittal views), mostly in the chin and lips areas. However, an important feature is the modifications in the vertical direction: a swelling of the cheeks is observed in patient #2, which the surgeons consider as completely coherent with a backward movement of the mandible.

However, the errors observed in the patient models (section 5.1.2) remains or are slightly increased. It is therefore difficult to evaluate the limitations due to the modeling aspects, since the shortcomings of the mesh conformation must be overcome first. Nevertheless, first results are considered very encouraging.

6 Discussion

The methodology presented in this paper is based on an atlas of the human face that is adapted to patient morphology, then used to simulate the aesthetic and functional consequences of surgical procedures.

Results in terms of precision, robustness and usability meet the requirements for the maxillofacial application. The generated models are considered to fit the patients morphologies, both numerically and according to several surgeons. The robustness of the patient model generation method was proven since it was successfully applied to six cases with different morphologies (skeletal class II and III, adults and children). Also, the results were not altered by image artefacts, and no additional pretreatment of the CT images were required. Although no quantitative validation was provided so far, the simulations of bone repositioning are considered very satisfying by the surgeons. An essential advantage of this method is it usability. Very few manual interactions are required, it is quite fast and robust. It seems therefore clearly compatible with a clinical use.

Although first results are satisfying and encouraging, both the quality of the atlas and the conformation procedure can be greatly improved to account for the different shortcomings pointed out by the clinicians. Then, a quantitative validation must be carried out, with facial measurements to validate the functional behavior of the model, and collection of patient data to compare simulated predictions with actual results of surgical procedures. The results of these experiments will then be used to improve the modeling from a mechanical point of view. Only these data will enable to find the most appropriate deformation modeling (elasticity in a small or large deformation framework, linear or non-linear stress/strain relationship, etc.) and to assess the range of mechanical parameters.

6.1 Model improvements

The generic face mesh can be greatly improved in many aspects. First, the mesh must be extended to the throat and neck, which is essential to enable throat contour studies, and eyes must be integrated. This should also greatly improve the graphical realism of the simulations.

Second, the muscles of mastication, which have an insertion on the mandible, must be added around the mouth and in the neck as they are directly affected by surgical procedure. Opening of the mouth, mastication and other jaw movements could thus be simulated. Muscles of the nose and the eyes also should be included in the model to improve the graphical realism of simulations.

Third, the 3D geometrical definition of the generic mesh should be improved, especially the muscles courses. The current mesh is composed of two layers representing the dermis and hypodermis. Muscles of the mouth were considered as completely inserted in the outer layer, whereas their course is much more complex, between the outer dermis and the facial bones. A solution would be not to use a layered mesh anymore, and designing a mesh integrating the real 3D geometry of each anatomical component. Although such a model would probably be much more accurate, we still believe that the amount of manual work to design it correctly is huge. Therefore, some improvements of the current layered mesh will be done. The important point is that the elements representing muscles are identified in the mesh, so that transverse isotropy properties can be defined. This task is really difficult to realize with an unstructured mesh. In the current version of the model, only elements in the outer layer of the mesh are considered to represent muscles. However, elements of both layers can be used. Indeed, the transverse isotropy direction does not have to be parallel to any of the element face. It can be defined with an angle in each element so that the modeled "fibers" start from the outer surface of the mesh in the corner of the lips, then run through the depth of the two mesh layers, to finish in the inner surface of the mesh, where the insertion in the bone is. Also, more layers could be added to integrate mastication muscles.

Another improvement in the face model concerns the modeling of contacts. Indeed, during simulations, collisions occur between upper and lower lips as well as between lips and teeth. Therefore, teeth have to be added via geometric boundary conditions, and all contacts must be detected and treated to prevent inter-penetration of the different parts of the mesh. Adding such constraints to take collisions into account and to prevent mesh penetration will be done using contacts elements in the Ansys^{TM}package (c.f. Ansys (1999)). This method could also be used to model the soft tissue sliding over the bone substructure, instead of using fixed contacts.

6.2   Conformation of the generic model to the patient

Although differences seems are not too large numerically (never more than 2mm), they are located in important morphological areas: nasal tip, nasolabial angle, maxillary and mandibular sulcus contour, lips contour, cheekbones contour. This important shortcoming, pointed out by the clinicians, has to be addressed. A first solution would be to use more information in the registration algorithm, like the surfaces normals. Another idea could be to determine a few feature points on the skin in the important morphological areas, which could be used to force the registration algorithm to better fit these areas. Also, the mesh could be refined in some coarse areas (like the cheeks) to give more elasticity to the mesh during the conformation to the patient morphology.

Adapting the generic model to the morphology of the patient is currently done in two steps. Nodes are fitted to the skin and skull surfaces segmented from CT images. Then, a post-treatment is applied to correct distorted elements. So far, these two procedures are independent. Registration is performed on a set of 3D points (the nodes of the mesh) without using any connectivity information between those points, i.e. the elements definition. A first improvement would be to integrate the connectivity knowledge in the matching algorithm, to prevent elements from shape distortions.

From a clinical point of view, a limitation of our patient FE mesh generation is the requirement of a CT exam for each patient. Data usually available are a small set of teleradiographies coupled with photography of the patient face. A 3D/2D registration algorithm that uses only data segmented on radiographies could be considered. However, with the decreasing invasivity of new scanners, CT is being more and more systematically used for this surgery.

Another shortcoming concerns the patient data used to conform the generic model. So far, only geometric information segmented from CT images is used. No information about patient soft tissue specificity is currently taken into account. A first issue is the location of the muscles on the face. The muscles course and insertions can greatly vary from person to person, especially in pathological subjects. As shown in figure 12, the inference of the patient muscle location resulting from the Mesh-Matching algorithm is coherent with a normal arrangement of the muscles in the face. However, the approximation of the patient muscles definition is still qualitative. Although this direction was not investigated so far, the use of MRI data seems really adapted to address that problem. Indeed, MRI offers quality information about the different facial soft tissues, especially fat and muscles since the pixels intensity of these tissue are really contrasted. For example, with a T1 ponderation, fat appears as high density pixels while low signal areas between the skull and skin surface correspond to face muscles. To our knowledge, few studies have already been carried out toward an automatic segmentation of fat and muscles in MRI images. From a general point of view, the use of a generic model integrating anatomical structures (muscles, nerves, blood vessels in an organ, etc) could be an interesting approach, to infer these structures locations as a starting point of a more complex segmentation procedure. A lot of work still has to be carried out in this promising direction before results can be integrated in our project. However, assuming specific information about patient muscles location is available, it could easily be integrated into the Mesh-Matching algorithm as feature-based constraints, in addition to the position and regularity criteria currently used in the disparity function of the elastic matching.

Other patient specific information could be the range of the patient face deformations induced by muscles. This has been partly addressed by Lucero and Munhall (1999), who measured facial mimics using a tracking system, in

parallel with EMG muscle activation recordings. Movements of the jaw could also be studied to characterize each patient range of motion. However, if such studies are really interesting, they are still currently difficult to use in a clinical routine procedure.

Finally, a last point would be to actually measure mechanical parameters of each patient. Indeed, it can be easily felt by palpation that the tissue elasticity greatly vary from person to person. However, considering the very small amount of data available in the literature and the complexity of the existing indentation methods, we are certainly far from a routine clinical use. Nevertheless, some methods are being developed, such as Magnetic Resonance Elastography (see for example Muthupillai et al., 1996) or Ultrasound studies.

6.3 Biomechanical modeling improvements

Two modeling assumptions can be made to approximate the behavior of face soft tissues with the Finite Element method.

A first modeling formulation is the linear-elasticity, which means that the stress/strain ratio is considered linear during soft tissue deformations. Within this framework, parameters are the Young modulus, namely the elasticity, and the Poisson's coefficient that indicates the compressibility of the tissues. Two computation methods are available, known as small or large deformations. In small deformation hypothesis, the second order term in the Green formula is ignored (Zienkiewicz and Taylor, 1989). As a consequence, the formulation can be written as a matrix inversion problem. Although this method is the less accurate, this is the most widely used in the literature of facial tissue deformation modeling because of its relatively easy implementation. Under the large displacement hypothesis, the second order term is not ignored, which leads to a more accurate approximation but seriously increases the computation complexity. To be very strict, small deformation method should not be used with a strain ratio above 3%. In practice, large deformation modeling is often chosen only for a strain ratio that exceeds 10 or 15%. Despite the relative inaccuracy of linear elastic modeling, this method is widely used in the literature and numerous computation software or libraries are available. Besides, computation time can be reduced using pre-calculus (Cotin et al., 1999). A large amount of Finite Element results (displacements, strains and stresses) are calculated and stored for displacements in every direction. Then, real-time analyses are computed through linear combinations of the stored values.

A second modeling framework is known as non-linear elasticity. Although its formulation is much more complicated than for linear elasticity, it is now included in most of the commercial Finite Element packages (like Ansys™,

Patran^{TM}, Abaqus^{TM}etc.), for isotropic materials only. Tissue behavior is characterized by the relationship between the stress and strain, which can be highly non linear and complex.

The first simulations presented in this paper were all computed in a linear-elastic framework. Although this method can be considered inadequate, it was preferred, in a first step, to stick with a simple mechanical modeling such as linear-elasticity. However, our model enables to take anisotropy into account which, to our knowledge, has never been addressed in the literature, and might be as important to consider as the mechanical non-linearity of the tissues.

It was also our choice not to focus on a complicated biomechanical modeling while real data are not available to validate the simulated soft tissue deformations. Indeed, non-linear simulations can be computed using Ansys^{TM}, but their accuracy in comparison to linear-elasticity simulations cannot be assessed without any real data. Hence, our approach was first to develop a method to automatically build a face model of each patient, integrating anatomical structures such as muscles. Simultaneously, our research team has been working on developing a complete Computer-Aided system for maxillofacial surgery applications. This latter point will enable us to acquire enough quality data (see next section) to assess the relevancy and the accuracy of our facial tissue deformation modeling. We will then, and only then, be able to compare different mechanical modeling approaches, being isotropic or anisotropic, with a linear or non-linear formulation. Finally, as a much more long-term perspective, issues related to soft tissue removal, sewing and swelling will have to be taken into account.

6.4   Quantitative protocol for clinical validation

Although a first qualitative validation has been presented, the method proposed in this paper has to be quantitatively validated. While it concerns current research, since no post-operative data are currently available (see section 4.2), the evaluation protocol is globally defined. This quantitative validation will be carried out as soon as quantitative post-operative data are available.

A first point concerns the validation of the algorithms proposed to automatically generate patient models. Pre-operative CT exams were acquired for six patients. These data were used to build face models presented in section 4, which has validated the feasibility and good accuracy of the model generation method. However, further investigations must be carried out especially to access the quality of the inferred location of the muscles on the patient face. As pointed out in section 6.2, MRI could be used for this particular study.

The presented face tissue modeling has always been developed in the frame-

work of Computer-Aided maxillofacial surgery. Hence, the main validation protocol will obviously rely on the clinical application itself. First, accurate surgical planning must be defined, either traditionally or using the software developed in our laboratory (Bettega et al., 2000). Afterwards, a navigation system must be developed to help the surgeon transferring its planning to the operating room. Before developing such a system, current research concerns a quantitative comparison method between pre and post-operative data to accurately measure the actual bone displacements performed by the surgeon. This information is useful for the clinician to evaluate the error between the actual surgical gesture and the planned one. Moreover, the measured bone displacements will be used as input to the patient face model to simulate tissue deformations resulting from the surgery. Then, simulated and real post-operative appearance will have to be quantitatively compared, for example using a generalized distance between the model and the post-operative skull and skin surfaces. Once these quantitative measurements will be available, different mechanical modeling assumptions could be evaluated to find out the most adapted framework.

Finally, the last validation concerns the functional behavior of the models. A first step will be to measure face deformations on healthy subjects. For example, specific facial mimics can be recorded using tracking systems, coupled with EMG muscle activation measurements (Lucero and Munhall, 1999). The muscle activation parameters could then be used as input of the face model and facial deformations compared with recorded data.

7   Conclusion

The method presented in this paper is based on a generic biomechanical model of the face soft tissues that is adapted to patient morphology, then used to simulate the aesthetic and functional consequences of surgical procedures.

The proposed patient model generation algorithm has given convincing results in terms of precision, robustness and usability. It seems therefore compatible with a use in current clinical practice. Although only a qualitative validation was provided, the simulations of soft tissue deformations following bones repositioning are considered very satisfying and encouraging by several specialized surgeons.

Future works concern both the generic model definition and the conformation procedure, to improve the patient model precision in face areas that are the most relevant for maxillofacial surgery. Then, a quantitative validation will be carried out, with facial measurements to validate the functional behavior of the model, and collection of post-operative patient data to compare simulated

predictions with the actual outcomes of surgical procedures. The results of these experiments will then be used to improve the modeling.

8 Acknowledgements

References

Ansys. *Ansys, Theory Reference*, 1999. release 5.6.

S. Barré, C. Fernandez, P. Paume, and G. Subrenat. Simulating Facial Surgery. In *Proc. of the IS&T/SPIE Electronic Imaging*, volume 3960, pages 334–345, 2000.

G. Bettega, V. Dessenne, P. Cinquin, and B. Raphäel. Computer assisted mandibular condyle positioning in orthognatic surgery. *J. of Oral Maxillofacial Surgery*, 54(5):553–558, 1996.

G. Bettega, Y. Payan, B. Mollard, A. Boyer, B. Raphäel, and S. Lavallée. A simulator for maxillo-facial surgery integrating cephalometry and orthodontia. *Journal of Computer Aided Surgery*, 5(3):156–165, 2000.

S. Cannan, M. Stephenson, and T. Blacker. Optismoothing : an optimization-driven approach to mesh smoothing. *Finite Elements in Analysis and Design*, 13:185–190, 1993.

S. Cotin, H. Delingette, and N. Ayache. Real-Time Elastic Deformations of Soft Tissues for Surgery Simulation. *IEEE Transactions on Visualization and Computer Graphics*, 5(1):62–73, 1999.

B. Couteau, Y. Payan, and S. Lavall/'ee. The Mesh-Matching algorithm : an automatic 3D mesh generator for finite element structures. *Journal of Biomechanics*, 33(8):1005–1009, 2000.

J.C. Craveur. *Modlisation des structures: Calcul par lments finis*. Masson, Paris, 1996. in french.

C. Cutting, F.L. Bookstein, B. Grayson, L. Fellingham, and J.G. Mc Carthy. Three-dimensional computer-assisted design of craniofacial surgical procedures : optimization and interaction with cephalometric and CT-based models. *Plastic Reconstruction Surgery*, 77(6):877–885, 1986.

J. Delaire. L'analyse architecturale et structurale cranio-faciale (de pro-

fil). Principes thoriques. Quelques exemples d'emploi en chirurgie maxillo-faciale. *Rev. Stomatol. Chirurgie Maxillo Faciale*, 79:1–33, 1978. in french.

H. Delingette, G. Subsol, S. Cotin, and J. Pignon. A craniofacial surgery simulation testbed. Technical Report 2199, INRIA, 1994.

F. A. Duck. *Physical properties of tissues: a comprehensive reference book.* Academic Press, London, 1990.

P. C. Everett, E. B. Selbin, M. Troulis, L. B. Kaban, and R. Kikinis. A 3-D system for planning and simulating minimally-invasive distraction osteogenesis of the facial skeleton. In *3rd Int. Conf. on Medical Image Computing and Computer Assi Intervention, MICCAI'2000*, volume 1935 of *LNCS*, pages 1029–1039. Springer, october 2000.

L.A. Freitag and P. Plassmann. Local optimization-based simplicial mesh untangling and improvement. *ANL/MCS*, 39:749–756, 1999.

Y. C. Fung. *Biomechanics: Mechanical Properties of Living Tissues.* Springer Verlag, New York, 1993.

E. Gladilin, S. Zachow, H.C. Hege, and P. Deuflard. FE-based heuristic approach for the estimation of person-specific facial mimics. In *5th International Symposium on Computer Methods in Biomechanics and Biomedical Engineering*, Roma, Italy, november 2001.

T. Guiard-Marigny, A. Adjoudani, and C. Benoit. 3D models of the lips and jaw for visual speech synthesis. In Van Stanten J.P.H., Sproat R.W., Olive J.P., and Hirschberg J., editors, *Progress in speech synthesis.* Springer-Verlag, New York, 1996.

W. J. Hardcastle. *Physiology of Speech Production.* Academic Press, London, 1976.

E. Keeve, S. Girod, and B. Girod. Computer-Aided Craniofacial Surgery. In H.U. Lemke and al., editors, *Computer Assisted Radiology*, pages 757–763. Elsevier Science B.V., 1996.

E. Keeve, S. Girod, R. Kikinis, and B. Girod. Deformable Modeling of Facial Tissue for Craniofacial Surgery Simulation. *Journal of Computer Aided Surgery*, 3:228–238, 1998.

T. Konno, H. Mitani, H. Chiyokura, and I. Tanaka. Surgical simulation of facial paralysis. *Health care in the information age*, pages 488–497, 1996.

Y. Lee, D. Terzopoulos, and K. Waters. Realistic Modeling for Facial Animation. In *SIGGRAPH'95*, pages 55–62, 1995.

L.J. Lo, J.L. Marsh, M.W. Vannier, and V.V. Patel. Craniofacial computer assisted surgical planning. *Clin. Plastic Surgery*, 21:501–516, 1994.

Lorensen. Marching cube: a High Resolution 3D Surface Construction Algorithm. *Computer Graphics, SIGGRAPH'87*, 21(4):163–169, 1987.

V. Luboz, B. Couteau, and Y. Payan. 3D finite element meshing of entire femora by using the mesh-matching algorithm. In *Proc. of Orthopaedic Research Society, ORS'2001*, 2001a.

V. Luboz, Y. Payan, P. Swider, and B. Couteau. Automatic 3D Finite Element Mesh Generation: Data Fitting for an Atlas. In *Proc. of 5th Int. Symposium on Computer Methods in Biomechanics and Biomedical Engineering,*

CMBBE'2001, 2001b.

J.C. Lucero and K.G. Munhall. A model of facial biomechanics for speech production. *J. Acoustic Soc. Am.*, 106(5):2834–2842, 1999.

Z. Mao, P. Sebert, and A.F. Ayoub. Development of 3D Measuring Techniques for the Analysis of Facial Soft Tissue Change. In *3rd Int. Conf. on Medical Image Computing and Computer Assi Intervention, MICCAI'2000*, volume 1935 of *LNCS*, pages 1051–1060. Springer, october 2000.

R. Marmulla and H. Niederdellmann. Surgical planning of computer-assisted repositioning osteotomies. *Plast. Reconst. Surg.*, 104:938–944, 1999.

J.L. Marsh, M.W. Vannier, S. Bresina, and K.M. Hemmer. Applications of computer graphics in craniofacial surgery. *Clin. Plast. Surg.*, 13(3):938–944, 1986.

R. Muthupillai, P.J. Rossman, D.J. Lomas, J.F. Greenleaf, S.J. Riederer, and R.L. Ehman. Resonance Imaging of Transverse Acoustic Strain Waves. *Magnetic Resonance in Medicine*, 36:266–274, 1996.

J. Ohayon, Y. Usson, P.S. Jouk, and H. Cai. Fibre orientation in human fetal heart and ventricular mechanics : a small perturbation analysis. *Computer Methods in Biomedical Engineering*, 2:83–105, 1999.

M. H. Gross R. M. Koch and A. A. Bosshard. Emotion Editing using Finite Element. *Eurographics'98*, 17(3), 1998.

M.S.H. Roth, M. Gross, S. Turello, and F.R. Carls. A Bernstein-Bzier based approach to soft tissue simulation. *Eurographics'98*, 17(3), 1998.

H. Rouvière and A. Delmas. *Anatomie humaine descriptive, topographique et fonctionnelle. Tome 1: Tête et cou.* Masson, Paris, 14 edition, 1997. in french.

A. Schramm, N.C. Gelldrich, R. Gutwald, J. Schipper, H. Bloss, H. Hustedt, R. Schmelzeisen, and J.E. Otten. Indications for computer-assisted treatment of cranio-maxillofacial tumors. *J. Computer Aided Surgery*, 5(5):343–352, 2000.

P. Schutyser, J. Van Cleynenbreugel, M. Ferrant, J. Schoenaers, and P. Suetens. Image-based 3D planning of maxillofacial distraction procedures including soft tissue implications. In *3rd Int. Conf. on Medical Image Computing and Computer Assi Intervention, MICCAI'2000*, volume 1935 of *LNCS*, pages 999–1007. Springer, october 2000.

R. Szeliski and S. Lavallee. Matching 3-D anatomical surfaces with non-rigid deformations u octree-splines. *Int. J. of Computer Vision*, 18(2):171–186, 1996.

M. Teschner, S. Girod, and B. Girod. Optimization approaches for soft-tissue prediction in craniofacial surgery simulation. In *2nd Int. Conf. on Medical Image Computing and Computer Assi Intervention, MICCAI'99*, volume 1679 of *LNCS*, pages 1183–1190. Springer, 1999.

G. Touzot and G. Dhatt. *Une reprsentation de la mthode des lments finis.* Collection universit de Compigne, 1976. in french.

J.K. Udupa and D. Odhner. Fast visualization, manipulation, and analysis of binary volumetric objects. *IEEE Computer Graphics and Applications*,

pages 53–62, 1991.

M.W. Vannier, J.L. Marsh, and A. Tsiaras. Craniofacial surgical planning and evaluation with computers. In R. Taylor, S. Lavallee, G. Burdea, and R. Mosges, editors, *Computer Integrated Surgery*, pages 673–677. MIT Press, Cambridge, MA, 1996.

K. Waters. Synthetic muscular contraction on facial tissue derived from computer tomography data. In R. Taylor, S. Lavallee, G. Burdea, and R. Mosges, editors, *Computer Integrated Surgery*, pages 191–200. MIT Press, Cambridge, MA, 1996.

J. Xia, N. Samman, C.K. Chua, R.W.K. Yeung, D. Wang, S.G. Shen, H.H.S. Ip, and H. Tideman. PC-based virtual reality simulation for orthognathic surgery. In *3rd Int. Conf. on Medical Image Computing and Computer Assi Intervention, MICCAI'2000*, volume 1935 of *LNCS*, pages 1019–1028. Springer, october 2000.

S. Zachow, E. Gladiline, H.C. Hege, and P. Deuflhard. Finite element simulation for soft tissue prediction. In H.U. Lemke and al., editors, *Computer Assisted Radiology and Surgery, CARS'00*, pages 23–28. Elsevier, 2000.

O.C. Zienkiewicz and R.L. Taylor. *The Finite Element Method. Basic formulation and linear problems.* MacGraw-Hill Book Company (UK) Limited, Maidenhead, 1989.